

# FATIGUE OF COMPOSITES UNDER SPECTRUM LOADING

**M. M. Ratwani**

*Northrop Corporation, One Northrop Avenue, Hawthorne, CA 90250, USA*

Manager, Strength and Life Assurance Research

Northrop Corporation  
One Northrop Avenue  
Hawthorne, California 90250

## ABSTRACT

Fatigue behavior of graphite/epoxy composite laminates under compression-dominated spectrum loading is discussed in this paper. It is shown that the damage accumulation under spectrum loading differs from that under constant amplitude loading.

The development of a nonlinear cumulative damage model based on delamination propagation is discussed. The model can be used reliably to predict the fatigue life of laminates in which interlaminar shear stresses are high and delamination propagation is the dominant failure mechanism. A residual strength prediction model, based on the combination of strength degradation model and delamination propagation theory, is discussed. Good correlation between experimentally observed residual strength data and predictions have been shown. The influences of spectrum variations on fatigue life are also discussed.

## KEYWORDS

Composites; delamination; fatigue; residual strength; spectrum loading; X-ray radiography.

## INTRODUCTION

Advanced fiber-reinforced composite materials are increasingly being utilized in aircraft to provide lighter weight and more durable structure than can be achieved with metallic structures. The fatigue behavior of composites under constant amplitude tension-tension, and tension-dominated spectrum loading has generally been extremely good and they far exceed the comparable behavior of metals. The experimental investigations in the past few years (References 1-9) indicate that, unlike metals, composites exhibit significant reduction in life under tension-compression and compression-compression loading as compared to tension-tension loading. The mechanism of failure has been observed to be local progressive fatigue failure of the matrix near a stress raiser,

resulting in fiber-split and progressive delaminations which cause eventual laminate failure. These data indicate that compressive loading is an important design consideration, and a detailed study under such a loading is needed. The fatigue life requirements of the presently used composite components have been satisfied by designing to relatively low strain levels and performing extensive specimen, subcomponent and full-scale fatigue tests to certify strength and durability. While this approach has been accepted in current composite designs, to fully utilize the weight saving potential of composites, improved fatigue analysis methods are required. Some of these methods are discussed in References 6 and 10 through 13.

A linear cumulative damage model, e.g. Miner's rule, is used as a basis for fatigue life prediction of metallic structures. The applicability of the linear cumulative damage model to composites has been found to be unconservative (Reference 1). A nonlinear cumulative damage model, based on delamination propagation, has been developed in References 11 through 12. This model has shown good correlation between predictions and test results for composite laminates in which the delamination propagation is the dominant failure mechanism.

The study of damage accumulation in composites under fatigue loads has been carried out in References 11 and 13 through 17. It is shown in Reference 16 that the damage growth in composite laminates depends on the stacking sequence. The experimental results of Reference 17 indicate that the damage accumulation direction and extent change with stress ratio, depending on the ply orientations and stacking sequence of the laminate.

The present paper deals with the fatigue behavior of graphite/epoxy composites under compression-dominated "blocked" and flight-by-flight spectrum loading. Damage accumulation, fatigue life and residual strength prediction models, and spectrum variation effects on fatigue life are also discussed in this paper.

#### DAMAGE ACCUMULATION IN COMPOSITES

The study of damage accumulation in composites under constant amplitude and spectrum loading has been carried out in References 11, 13, 16-17. Two specimen configurations shown in Figures 1 and 2 have been used in these investigations. Specimen configuration 1 has a short test area and does not need any antibuckling guides during testing, whereas specimen configuration 2 needs lateral supports. The damage growth in configuration 1 specimens is restricted due to the short test area, and damage grows into the tab area prior to failure. Configuration 2 specimen damage growth is influenced by the antibuckling guides and may be retarded due to the clamping effect produced by the guides.

The spectrum fatigue tests in References 11-12, 16-17 have been carried out under blocked and flight-by-flight fighter aircraft spectrum loadings. The compression-dominated blocked spectrum loading used in the tests is shown in Fig. 3.

#### Specimen Fabrication

All specimens were fabricated from AS/3501-6 graphite/epoxy unidirectional tape prepreg (single-ply with a nominal thickness of 0.0055 inch (0.140 mm)). Prior to machining the individual test specimens from fabricated panels,

every panel was subjected to nondestructive inspection (NDI) to assure that all test specimens were free of fabrication defects. Ultrasonic C-scan records were obtained for the panels after cure and before bonding of tabs and machining. The results of NDI showed the quality of the fabricated panels to be very good. Eight-ply 8517 glass/epoxy tabs were subsequently bonded to the panels with AF143 adhesive. Individual specimens were machined from these panels.

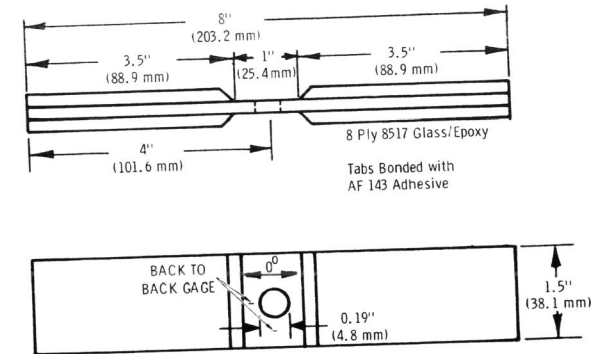


Fig. 1. Specimen configuration 1.

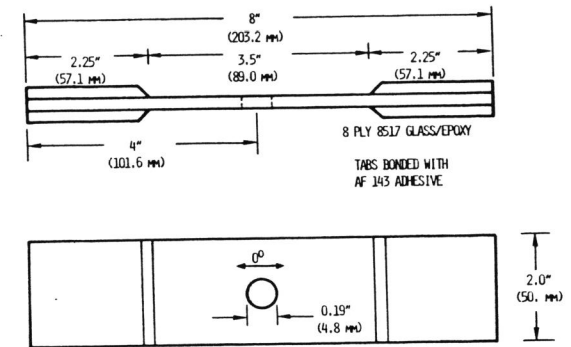


Fig. 2. Specimen configuration 2.

#### Specimen Testing

All fatigue tests were performed in MTS machines in a room temperature ambient environment. The specimens were gripped to avoid any out-of-plane bending. Initial specimens were strain-gaged back-to-back to check out the test fixture and to make sure that the strain gage readings on back-to-back gages did not differ by more than 5 percent.

#### Nondestructive Inspection (NDI) of Specimens

Test specimens were subjected to nondestructive inspection (NDI) at certain intervals of fatigue cycles. X-ray radiography with diiodobutane (DIB) was

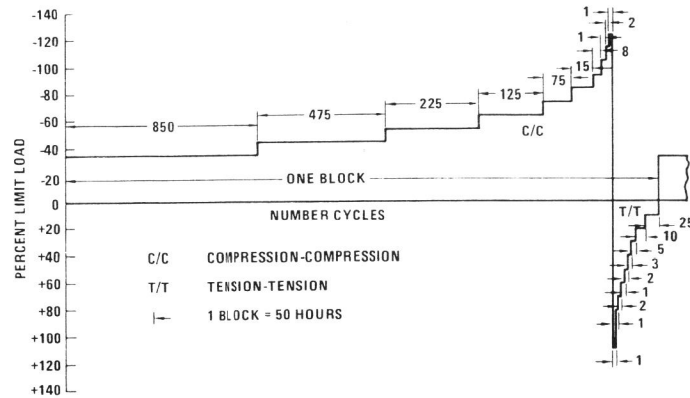


Fig. 3. Loading sequence used in spectrum fatigue loading

used to determine the extent of damage. The specimens were removed from the test machine at regular intervals and subjected to X-ray radiography. Diiodobutane (DIB) was carefully applied to edges of interest, with care being taken that it did not splatter on the faces of the specimens. Within two hours of the application of DIB, the specimens were exposed in the HP804 X-ray cabinet. Kodak film type AA was used for the X-ray record.

Damage Growth in 16-ply  $(0/+45/90/0_2/+45)_s$  Laminate 1  
(Specimen Configuration 1)

X-ray radiography of a laminate 1  $(0/+45/90/0_2/+45)_s$  specimen, tested at  $R$  (minimum stress to maximum stress ratio) = -1 and  $\sigma_{min} = -62.0$  ksi (-427 MPa), is shown in Fig. 4. The average notched compression static strength of this laminate is -66.9 ksi (-461 MPa). The X-ray radiography was taken after 300 and 800 cycles. The specimen failed after 840 cycles. It is seen that the delamination initiates around the hole at right angles to the loading direction. The delamination subsequently grows around the periphery of the hole and in the loading direction. Major growth takes place along the loading direction. Prior to failure, after 840 cycles, considerable cracking is observed in the laminate. Figure 5 shows X-ray radiography of the same laminate specimen tested at  $R = -\infty$  and  $\sigma_{min} = -51.5$  ksi (-355 MPa). The X-ray radiography pictures are shown after 150,000; 400,000; and 1,000,000 fatigue cycles. The specimen failed at 2,111,000 cycles. The delamination growth at  $R = -\infty$  is similar to that in specimens tested at  $R = -1.0$ . The delamination starts growing all around the edge of the hole and propagates along the loading direction. At 400,000 cycles the entire length of the test area is delaminated. However, the damage is confined to a narrow strip, extending on either side of the hole. The width of the damaged strip after 400,000 cycles and 1,000,000 cycles are almost the same.

X-ray radiography of four unfailed specimens, tested under blocked spectrum loading (Fig. 3), is shown in Fig. 6. It is seen that the width of the

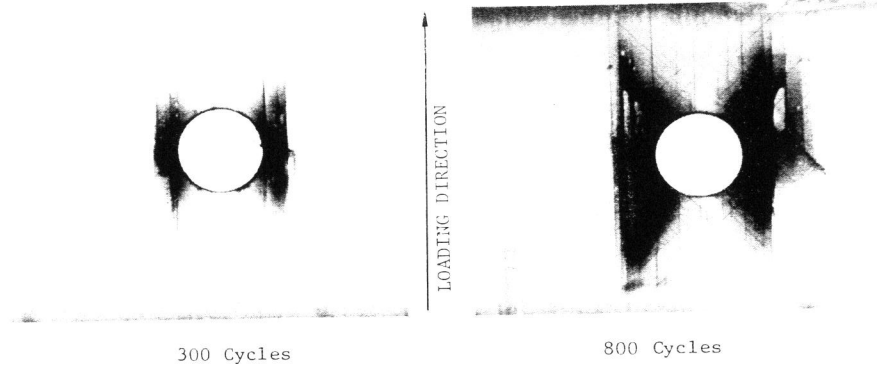


Fig. 4. X-ray radiography of  $(0/+45/90/0_2/+45)_s$  laminate specimen tested at  $R = -1$ ,  $\sigma_{min} = -62$  ksi (-427 MPa). Specimen failed at 840 cycles.

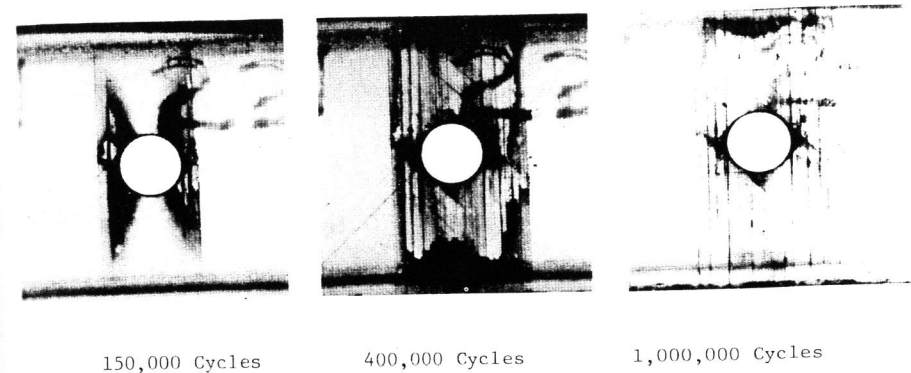


Fig. 5. X-ray radiograph of  $(0/+45/90/0_2/+45)_s$  laminate specimen tested at  $R = -\infty$ ,  $\sigma_{min} = -51.5$  ksi (-355 MPa). Specimen failed at 2,111,000 cycles.

damage band under spectrum loading (Fig. 6d) is larger than the damage zone prior to failure in specimens tested under constant amplitude loading.

Damage Growth in 16-ply  $(90/+45/0_3/+45)_s$  Laminate 2  
(Specimen Configuration 1)

X-ray radiography of a laminate 2  $(90/+45/0_3/+45)_s$  specimen tested at  $R = -1$ ,

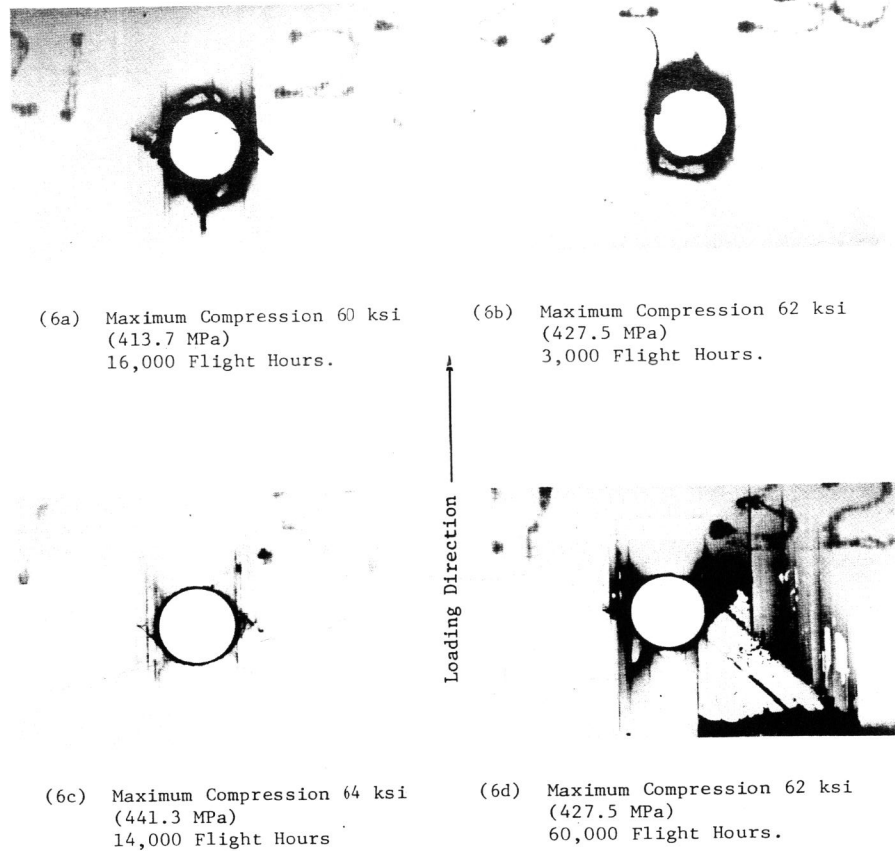


Fig. 6. X-ray radiography of  $(0/+45/90/0_2/+45)_s$  laminate specimens tested under blocked spectrum loading.

$\sigma_{\min} = -45.5$  ksi ( $-314$  MPa) is shown in Fig. 7. The X-ray radiography was taken after 20,000; 50,000; and 100,000 cycles. The specimen failed after 103,420 cycles. The figure indicates that the delamination propagates both in the radial direction and the axial (loading) direction. The delamination in the loading direction is confined to a narrow strip with width equal to the hole diameter and grows in the loading direction. The radial delamination initiates from the edge of the hole around its periphery and propagates radially. Prior to failure (at 100,000 cycles) the entire test area is delaminated as shown in the figure.

It may be noted that laminates 1 and 2 have the same percentages of 0,  $\pm 45$

and 90 degree plies and that only the stacking sequence has been changed. The damage growth under constant amplitude loading at  $R = -1$  for the two laminates is entirely different (Figures 4 and 7), indicating that the damage growth behavior in composites is influenced by stacking sequences.

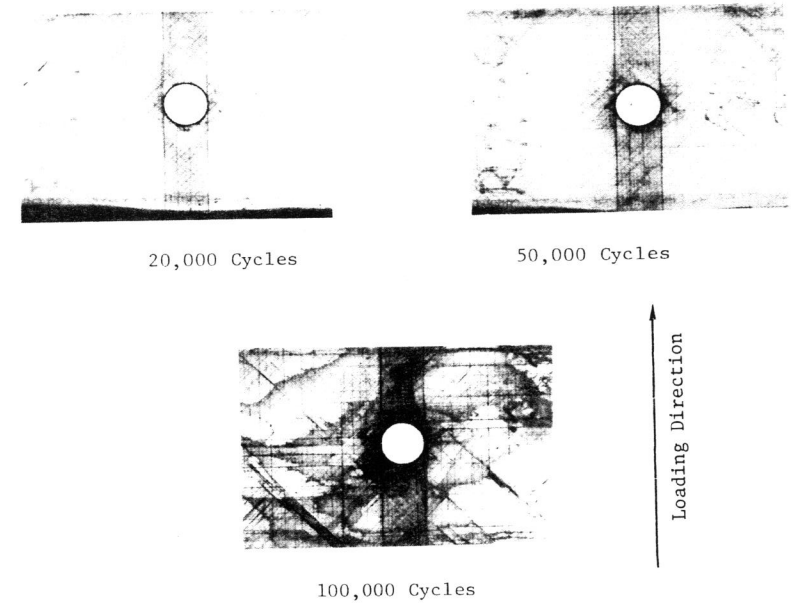


Fig. 7. X-ray radiography of  $(90/+45/0_3/+45)_s$  specimen laminate tested at  $R = -1$ ,  $\sigma_{\min} = -45.5$  ksi ( $-314$  MPa). Specimen failed at 103,420 cycles.

X-ray radiography of two unfailed specimens, tested under blocked spectrum loading (Fig. 3) is shown in Fig. 8. Very little damage is observed around the hole even after 20,000 flight hours of spectrum loading.

#### Damage Growth in 16-ply $(+45/0_4/90/0)_s$ Laminate 3 (Specimen Configuration 2)

X-ray radiography of laminate 3,  $(+45/0_4/90/0)_s$  specimen (configuration 2) tested at  $R$  (minimum to maximum stress ratio) =  $-\infty$  and a minimum stress ( $\sigma_{\min}$ ) of  $-60.0$  ksi ( $-413.7$  MPa) is shown in Fig. 9. The X-ray radiographs are shown after 1,000; 2,000; 15,000; 50,000; 700,000 and 1,900,000 cycles. It is seen that the damage initiated around the hole (Fig. 9a) and then started growing along the loading direction (Fig. 9b). At 15,000 cycles, (Fig. 9c), the damage started growing at right angles to the loading



(8a) Maximum Compression 60 ksi (413.7 MPa)  
20,000 Flight Hours.

(8b) Maximum Compression 63 ksi (434.4 MPa)  
20,000 Flight Hours.

Fig. 8. X-ray radiography of  $(90/+45/0_3/+45)_s$  specimens tested under blocked spectrum loading

direction. Intermediate radiographs taken at 3,000; 4,000; 5,000; 6,000 and 8,000 cycles did not indicate much change in the size of the damage zone as compared to that at 2,000 cycles; however the density of matrix cracks in  $+45$  degree plies gradually increased. The damage zone along and perpendicular to the loading direction and the density of matrix cracks continued to increase with further application of fatigue cycles (Fig. 9d, e) up to about 1,000,000 cycles. No significant increase in damage zone size occurred with further increase in fatigue loading to 1,900,000 cycles (Fig. 9f).

X-ray radiography of laminate 3 specimen (configuration 2) tested at  $R = -1$  and  $\sigma_{min} = -60.0$  ksi ( $-413.7$  MPa) is shown in Fig. 10. The X-ray radiographs

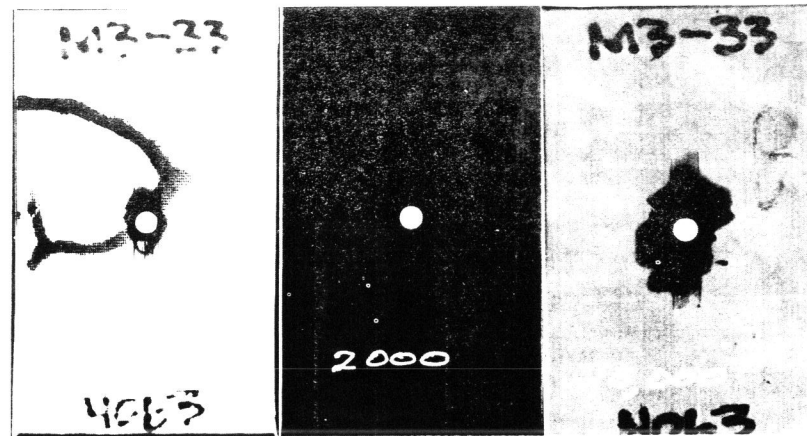
are shown after 500; 5,500; 10,000; 20,000; 50,000 and 100,000 cycles. The specimen failed after 100,390 cycles. The radiographs indicate the damage to have grown predominantly along the loading direction. The damage is confined to a narrow strip on either side of the hole with strip width equal to the hole diameter. The length of the strip equals the length of the specimen. The damage growth is different from that in the specimen tested at  $R = -\infty$  (Fig. 9), where the damage did not propagate throughout the length of the specimen and the growth was observed both along and perpendicular to the loading direction (Fig. 9).

It may be noted that the direction of damage growth in laminate 1 is not influenced by R-ratio, but in laminate 3 it is influenced by the R-ratio.

#### FATIGUE LIFE PREDICTION

##### Delamination Propagation Model

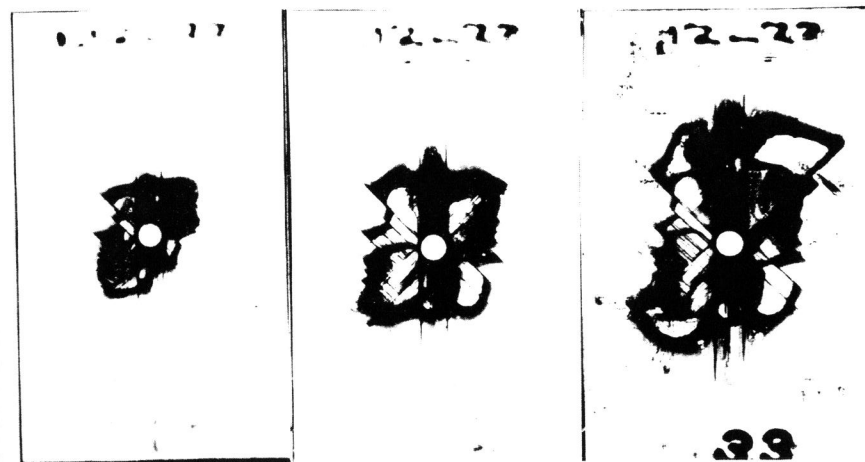
A macromechanics model, based on the delamination between plies was developed in Reference 10 for fatigue life prediction. The model is based on the assumption that initial defects of macroscopic levels exist in the composite between plies. During fatigue loads, the defects along the free edge or around a stress raiser are opened by induced interlaminar shear and/or normal



(9a) 1,000 Cycles

(9b) 2,000 Cycles

(9c) 15,000 Cycles

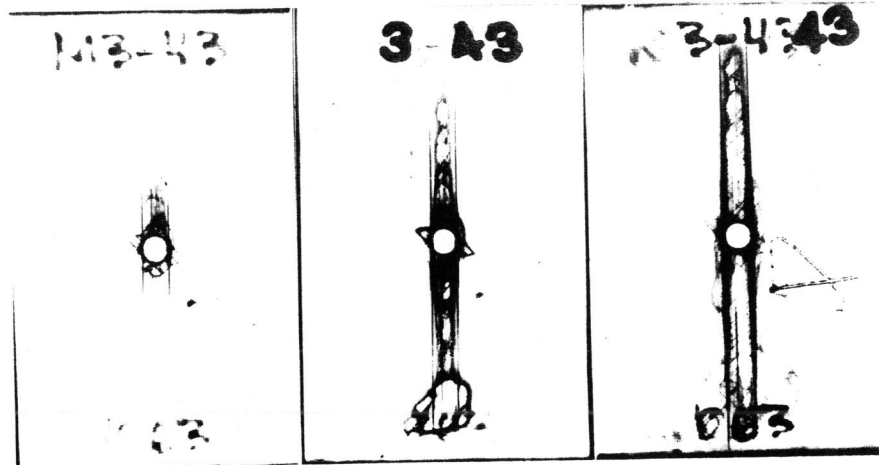


(9d) 50,000 Cycles

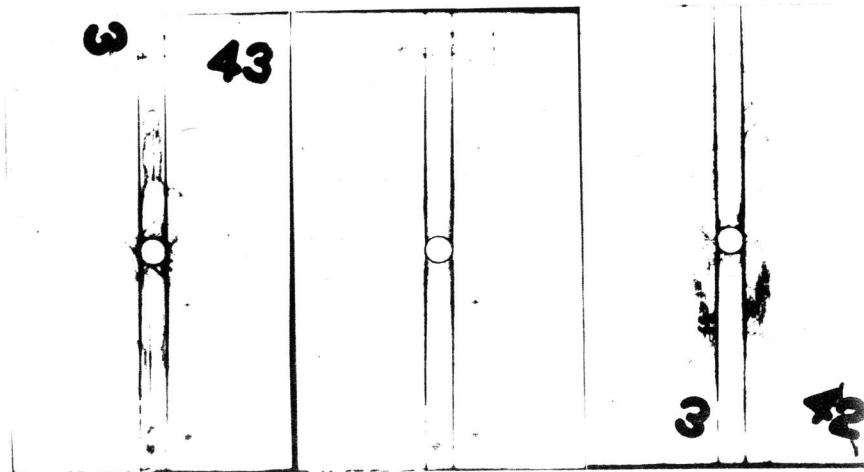
(9e) 700,000 Cycles

(9f) 1,900,000 Cycles

Fig. 9. X-ray radiography of  $(+45/0_4/90/0)_s$  laminate specimen (configuration 2) tested at  $R = -\infty$  and  $\sigma_{min} = -60.0$  ksi ( $-413.7$  MPa).



(10a) 500 Cycles (10b) 5,500 Cycles (10c) 10,000 Cycles



(10d) 20,000 Cycles (10e) 50,000 Cycles (10f) 100,000 Cycles

Fig. 10. X-ray radiography of  $(+45/0_4/90/0)_s$  laminate specimen (configuration 1), tested at  $R = -1.0$  and  $\sigma_{min} = -60.0$  ksi  $(-413.7$  MPa).

stresses. During fatigue cycling, these defects propagate causing progressive delamination of the composite. When the delamination reaches a critical size, buckling of a composite lamina or group of lamina--that have separated from the total laminate--will take place, causing the collapse of the structure.

Consider the composite laminate with a hole subjected to compressive fatigue loads, as shown in Fig. 11. If the load level is sufficiently large, delaminations will initiate between plies in which the interlaminar shear stresses are large and normal stresses are tensile. However, one of the delaminations will grow dominantly and govern the final failure of the laminate. The expected location of the dominant delamination can be obtained by analysis of interlaminar stresses. In Fig. 11, the dominant delamination is assumed to propagate between the first and second plies. It is assumed that there exists a threshold stress below which delamination will not initiate or propagate. This phenomenon of threshold stress at which delamination does not propagate has been observed in References 2 and 10.

During fatigue loading the delamination propagates. When the length of delamination  $b$ , as shown in Fig. 11 reaches a critical value  $b_c$ , the outer lamina (first-ply in Fig. 11) will buckle during compression excursion of the load at minimum applied stress  $\sigma_{min}$  in the fatigue loading, and will result in the collapse of the panel. The final failure is due to buckling, and hence the size of the dominant delamination will depend on the maximum compressive stress. The value of critical delamination  $b_c$  will be smaller for a larger compressive load. This is substantiated by the experimental results of Reference 2, where it was observed that the size of the delamination at failure was small for large compressive loads, and vice versa.

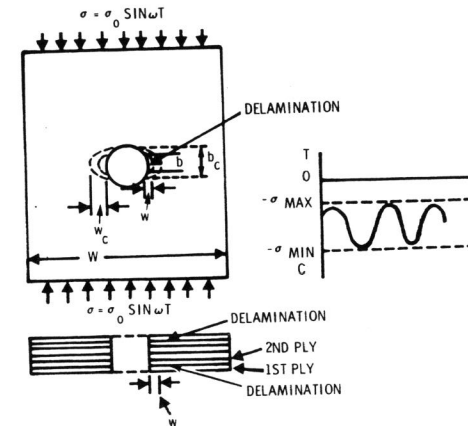


Fig. 11. Composite panel subjected to fatigue loads

The delamination propagation model is given by (Reference 10)

$$\frac{db}{dN} = C_1 (\tau_{zma} - \tau_{zmi} - \tau_{th})^{n_1} b^{m_1} \quad (1)$$

where

- b is the length of the delamination
- N is the number of fatigue cycles
- $\tau_{zmi}$  is the minimum interlaminar shear stress
- $\tau_{zma}$  is the maximum interlaminar shear stress
- $\tau_{th}$  is the interlaminar threshold shear stress range
- $C_1, n_1$  and  $m_1$  are constants and will depend on the resin system

It was shown in Reference 10 that for AS/3501-6 resin system ( $n_1 = 5, m_1 = 2.5$ ), the delamination propagation Equation (1) can be integrated to obtain

$$N_f = C \frac{\frac{1}{b_o^{1.5}} - \frac{1}{b_c^{1.5}}}{(\tau_{zma} - \tau_{zmi} - \tau_{tn})^5} \quad (2)$$

where  $b_o$  is the initial flaw size

$b_c$  is critical delamination size at failure, obtained by using the simple Euler equation (Reference 10).

C is a constant;  $C = 3.1 \times 10^3$  for AS/3501-6 resin and  $2.1 \times 10^4$  for Fiberite 934 resin.

Verification of the Delamination Propagation Model

The analytical fatigue life prediction model correlates fatigue life with interlaminar stresses. In order to predict fatigue life, interlaminar stresses have to be determined. The NASTRAN finite-element computer program was used to determine such interlaminar stresses in various laminates.

The fatigue data on the AS/3501-6 resin system have been analyzed in Reference 10. These data have been obtained on laminates with and without holes at different values of R (minimum to maximum stress) ratios on specimens with different width W. The interlaminar stress analysis of all the laminates was carried out, and the fatigue data have been plotted as a function of interlaminar shear stress range in Fig. 12. It is seen that the fatigue data lie within a scatterband, as expected for composites. The scatter is larger at high stress levels due to the influence of interlaminar normal stresses.

The fatigue life prediction model was also verified with the experimental data on the  $(+45/90_2/+45/90_2)_s$  laminate. These data have been obtained with the specimens shown in Fig. 1, using AS/3501-6 resin, under constant amplitude loading at  $R = -\infty$  and  $-1.0$ . A comparison of experimental and predicted fatigue life, assuming initial flaw sizes of 0.13 and 0.25 mm (0.005 and 0.01 in.) is shown in Fig. 13. The agreement between analytical predictions and experimental results is very good.

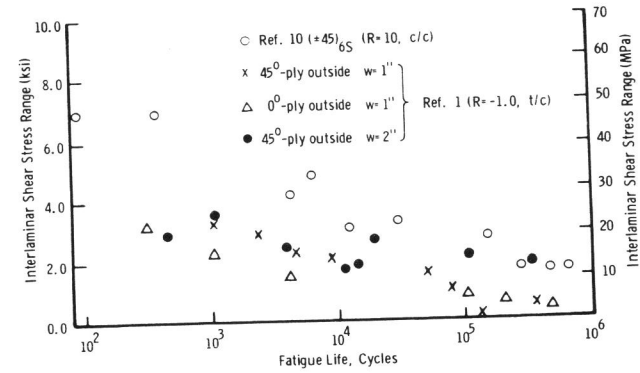


Fig. 12. Fatigue life vs. interlaminar shear stress range for laminates using AS/3501-6 resin system.

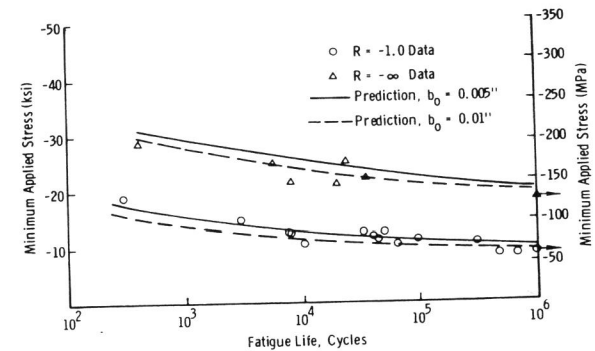


Fig. 13. Comparison of observed and predicted fatigue life of  $(+45/90_2/+45/90_2)_s$  laminate (AS/3501-6 resin,  $R = -1.0, -\infty$ ).

Cumulative Damage Model

The delamination propagation model given by Equation 1 is now applied to predict fatigue life under spectrum loading. Consider a composite laminate subjected to spectrum loading such as shown schematically in Fig. 14. The spectrum loading consists of cycles  $N_1, N_2, \dots, N_n$  each at a corresponding maximum stress of  $\sigma_{max1}, \sigma_{max2}, \dots, \sigma_{maxn}$  and a minimum stress of  $\sigma_{min1}, \sigma_{min2}, \dots, \sigma_{minn}$ .

Let the delamination propagate from initial size  $b_o$  to  $b_1$  during  $N_1$  cycles,

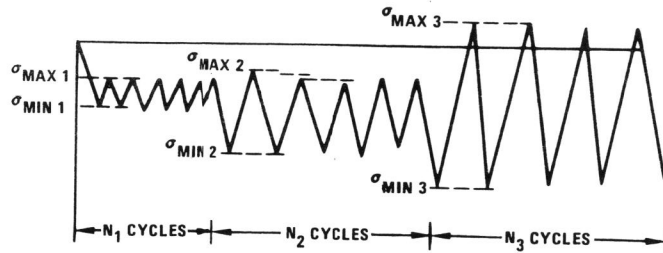


Fig. 14. Schematic of a compression-dominated spectrum.

from  $b_1$  to  $b_2$  during  $N_2$  cycles ... from  $b_{n-1}$  to  $b_n$  during  $N_n$  cycles.

The values of the critical delamination size,  $b_c$ , for each loading condition ( $\sigma_{min}$ ) can be obtained from the Euler equation, as given in Reference 10.

Let  $b_{c1}$ ,  $b_{c2}$  ...  $b_{cn}$  be the critical delamination sizes for each stress condition and  $N_{fi}$  be the cycles-to-failure for each stress condition under constant amplitude loading. The value of  $N_{fi}$  for each stress condition can be obtained from Equation (2) if the interlaminar stresses for each loading condition are known.

Let the interlaminar shear stress  $\tau$  be  $\alpha$  times the applied remote stress for the laminate under consideration. Integration of Equation (1) for each loading sequence gives

$$N_1 \left[ \alpha(\sigma_{max1} - \sigma_{min1}) - \tau_{th} \right]^{n_1} = C \left[ \frac{1}{b_o^{m-1}} - \frac{1}{b_1^{m-1}} \right], b_1 < b_{c1} \quad (3)$$

$$N_n \left[ \alpha(\sigma_{maxn} - \sigma_{minn}) - \tau_{th} \right]^{n_1} = C \left[ \frac{1}{b_{n-1}^{m-1}} - \frac{1}{b_n^{m-1}} \right], b_{n-1} < b_{cn}$$

A representation of total damage is obtained by adding the preceding equations, which results in

$$\sum N_i \left[ \alpha(\sigma_{maxi} - \sigma_{mini}) - \tau_{th} \right]^{n_1} = C \left[ \frac{1}{b_o^{m-1}} - \frac{1}{b_n^{m-1}} \right] \quad (4)$$

At failure  $b_n = b_{cn}$ , so that

$$\sum N_i \left[ \alpha(\sigma_{maxi} - \sigma_{mini}) - \tau_{th} \right]^{n_1} = C \left[ \frac{1}{b_o^{m-1}} - \frac{1}{b_{cn}^{m-1}} \right] \quad (5)$$

But

$$N_{fi} \left[ \alpha(\sigma_{maxi} - \sigma_{mini}) - \tau_{th} \right]^{n_1} = C \left[ \frac{1}{b_o^{m-1}} - \frac{1}{b_{ci}^{m-1}} \right] \quad (6)$$

where,  $N_{fi}$  is number of cycles to failure corresponding to the loading in the  $i^{\text{th}}$  block.

Substituting Equation (6) in Equation (5) gives

$$\left( \sum \frac{N_i}{N_{fi}} - 1 \right) \frac{1}{b_o^{m-1}} + \frac{1}{b_{cn}^{m-1}} - \sum \frac{N_i}{N_{fi} b_{ci}^{m-1}} = 0 \quad (7)$$

$$\sum \frac{N_i}{N_{fi}} \left[ 1 - \left( \frac{b_o}{b_{ci}} \right)^{m-1} \right] + \left( \frac{b_o}{b_{cn}} \right)^{m-1} = 1 \quad (8)$$

Equation (8) describes the cumulative damage model. It may be noted that the cumulative damage model based on Miner's rule is given by

$$\sum \frac{N_i}{N_{fi}} = 1 \quad (9)$$

The cumulative damage model based on delamination propagation, Equation (8), differs from that given by Miner's rule in that it has a nonlinear term which takes into consideration the delamination existing during each load sequence.

A computer program has been written in Reference 12 to predict fatigue life based on cumulative damage as given by Equation (8).

#### Verification of Cumulative Damage Model

Fatigue data under blocked spectrum loading (Fig. 3) were obtained on  $(+45/90_2/+45/90_2)_s$  laminate (Reference 9). A comparison of observed and predicted fatigue life, assuming two different initial flaw sizes, is shown in Fig. 15. It is seen that the fatigue life thus predicted correlated well with the observed life.

Experimental data on  $(0/+45/90/0_2/+45)_s$  and  $(90/+45/0_3/+45)_s$  laminates under compression-dominated block spectrum loading (Fig. 3) did not show failures in 3 lifetimes, up to a minimum stress level of -63 ksi (-434.4 MPa). Failures occurred at stress levels of -64 ksi (-441.3 MPa) and higher values. The static strength of the laminates with a hole was found to be between -62.5 ksi (-430.9 MPa) and -70.0 ksi (-482.4 MPa). The failure observed at -64 ksi (-441.3 MPa) were not fatigue failures but were quasi-static failures.

The experimental data on the  $(+45/0_4/90/0)$  laminate under typical spectrum loading (Reference 12) did not indicate any fatigue failures up to a minimum



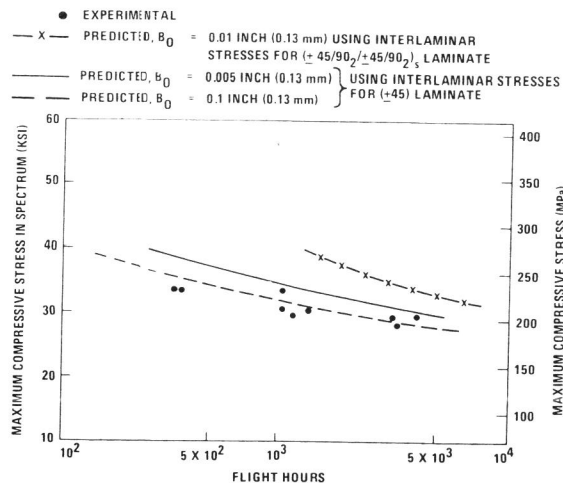


Fig. 15. Comparison of observed and predicted fatigue life of the  $(+45/90_2/+45/90_2)_s$  laminate under spectrum loading.

stress of -76.5 ksi (-527 MPa) at the end of 4 lifetimes (24,000 hours).

The majority of the loads in the spectrum are low amplitude loads and do not contribute to the delamination propagation. The majority of these low loads causes matrix damage which eventually reduces the delamination threshold of the resin, thereby reducing fatigue life.

RESIDUAL STRENGTH PREDICTION

A model for predicting compression residual strength of composites, subjected to compression fatigue loading has been developed in Reference 12. The model is based on the combination of a strength degradation model and the delamination propagation theory.

The residual strength of a laminate at any time during the fatigue process is assumed to be a function of the initial static laminate strength and the delamination size,  $b$  (in the loading direction), produced during the fatigue process. Furthermore, it is assumed that the residual strength at any time may be expressed as

$$R(N) = R(0)\phi(b_N) \tag{10}$$

where  $R(N)$  is the residual strength after  $N$  cycles of fatigue loading,  $R(0)$  is the static strength, and  $\phi(b_N)$  is an arbitrary function of the delamination size,  $b_N$ , produced during  $N$  number of fatigue cycles. It was shown in Reference 12 that the residual strength of a laminate is given by

$$R(N) = R(0) \left[ 1 - \left( 1 - \frac{\sigma_{\min}}{R(0)} \right) \left( \frac{b_N - b_0}{b_c - b_0} \right) \right] \tag{11}$$

where,

- $b_0$  = Initial flaw size
- $b_N$  = Delamination size produced during fatigue loading
- $b_c$  = Critical delamination size corresponding to the minimum stress in the flight (Reference 10)
- $\sigma_{\min}$  = Minimum stress in the fatigue loading in a particular flight.

Under blocked loading, shown in Fig. 14, the delamination size  $b_N$  is given by (Reference 12)

$$b_N = \frac{b_0}{\left[ \left( 1 - \sum \frac{N_i}{N_{fi}} \right) + \sum \frac{N_i}{N_{fi}} \left( \frac{b_0}{b_{ci}} \right)^{1.5} \right]^{0.67}} \tag{12}$$

where,

- $N_i$  is the number of fatigue cycles in  $i^{\text{th}}$  block
- $N_{fi}$  is the fatigue cycles to failure corresponding to the stresses in the  $i^{\text{th}}$  block
- $b_{ci}$  is the critical delamination size corresponding to the minimum stress in the  $i^{\text{th}}$  block.

The delamination size for a flight-by-flight spectrum can be computed from Equation (12) by carrying out the summation for each cycle. A computer program was developed in Reference 12 to obtain residual strength of composites under flight-by-flight spectrum loading.

The comparisons between observed and predicted residual strength of 16-ply  $(+45/0_4/90/0)_s$  laminate specimens, fatigued under compression-dominated flight-by-flight spectrum loading, at minimum stresses of -75 ksi (-517 MPa) and -76.5 ksi (-527 MPa), are shown in Figures 16 and 17. The comparison between observed and predicted residual strength is fairly good in view of the observed scatter in fatigue life (Reference 12).

SPECTRUM VARIATION EFFECTS

The influence of spectrum variation on fatigue life of composites has been investigated in References 18 and 19. The test data on  $(45/0/-45/90)_{2s}$  laminate in Reference 18, indicate that the spectrum truncation at either

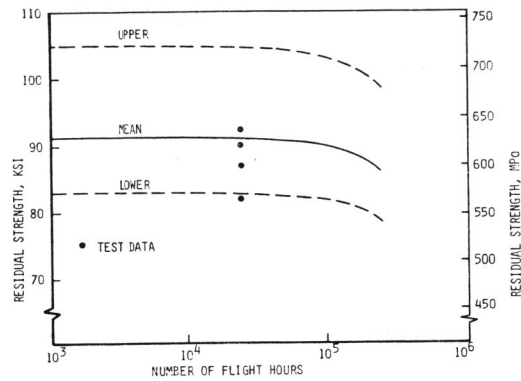


Fig. 16. 16-ply  $(+45/0_4/90/0)_s$  laminate under spectrum loading at a minimum stress of  $-75$  ksi ( $-517$  MPa).

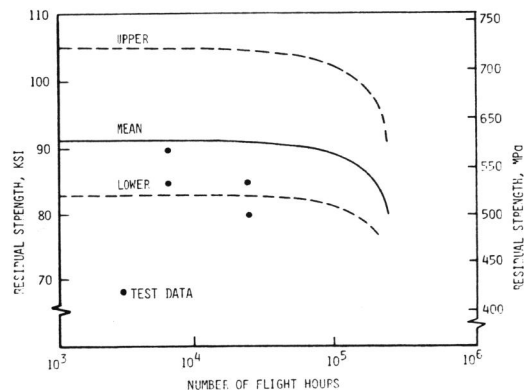


Fig. 17. 16-ply  $(+45/0_4/90/0)_s$  laminate under spectrum loading at a minimum stress of  $-76.5$  ksi ( $-527$  MPa).

the high- or low-load end of the spectrum produced lives greater than those obtained in the baseline complete-spectrum test. However, life was much more sensitive to truncations at the high-load end.

The test results on two laminates (fiber-dominated and matrix-dominated) in Reference 19 indicate that the removal of loads less than 55 percent of the limit load (reducing the number of load points from 18,000 to 5,000 per 1000 flight hours) almost doubled the fatigue life of the laminates. Addition of one overload (115 percent of test limit load for fiber-dominated laminate and 125 percent for matrix-dominated laminate) reduce life of the fiber-dominated laminate by a factor of 47 and that of matrix-dominated one by a factor of 24.

The above observations are consistent with the predictions from the

delamination propagation model. Addition of high loads contributes directly to the delamination propagation and results in shorter life, whereas the addition of low loads does not contribute to the delamination propagation but causes matrix damage. The matrix damage eventually influences the delamination growth rate by reducing the delamination threshold. Thus, the effect of low loads is less severe than that of high loads.

#### CONCLUDING REMARKS

Damage growth in composites is influenced by stacking sequence and ply orientations. The location of damage growth changes with stress ratio depending upon the type of laminate. Damage growth under spectrum loading differs significantly from that under constant amplitude loading. Composites exhibit large fatigue life, and under typical spectrum loading the fatigue failures do not occur at normal operating stress levels. The fatigue life of composites can be related to the interlaminar shear stresses produced in the laminate. Available delamination propagation models can be used to predict fatigue life of laminates in which delamination propagation is the dominant failure mechanism and takes place predominantly under interlaminar shear stresses.

#### ACKNOWLEDGMENT

The majority of work reported here was performed under contracts from Naval Air Development Center, Warminster, Pennsylvania, USA. Special thanks to Mr. L. Gause for valuable suggestions during the course of investigations. A part of the research was conducted under Northrop's Independent Research and Development Program.

#### REFERENCES

- Rosenfeld, M. S., and S. L. Huang (1978). Fatigue characteristics of graphite/epoxy laminates under compression loading. *J. Aircraft*, Vol. 15, No. 5, 264-268.
- Ryder, J. T., and E. K. Walker (1977). Effect of compression on fatigue properties of a quasi-isotropic graphite/epoxy composite. *Fatigue of Filamentary Composite Materials*. ASTM STP 636.
- Roderick, G. L.; and J. D. Whitcomb (1977). Fatigue damage of notched boron/epoxy laminates under constant amplitude loading. *Fatigue of Filamentary Composite Materials*. ASTM STP 636, 73-88.
- Ramani, S. V., and D. P. Williams (1976). Axial fatigue of  $0/+30)_{6s}$  graphite/epoxy. *Failure Modes in Composites III*, Metallurgical Society of the American Institute of Mining Engineers, 115-140.
- Ramani, S. V., and D. L. Williams (1977). Notched and unnotched fatigue behavior of angle-ply graphite/epoxy composites. *Fatigue of Filamentary Composite Materials*. ASTM STP 636, 27-46.
- Ramkumar, R. L., S. V. Kulkarni, and R. B. Pipes (1978). Evaluation and expansion of an analytical model for fatigue of notched composite laminates. *NASA CR-145308*.
- Kunz, S. C., and P. W. Beaumont (1975). Microcrack growth in graphite fiber-epoxy resin systems during compressive fatigue. *Fatigue of Filamentary Composite Materials*. ASTM STP 569, 71-91.
- Grimes, G. C., and D. F. Adams (1979). Investigation of compression fatigue properties of advanced composites. *Technical Report*, Prepared for Naval Air Systems Command by Northrop Corporation.

9. Kan, H. P., and M. M. Ratwani (1981). Compression fatigue behavior of composites. SAMPE quarterly, 10-14.
10. Ratwani, M. M., and H. P. Kan (1981). Compression fatigue analysis of fiber composites. J. Aircraft, Vol. 18, No. 6.
11. Ratwani, M. M., and H. P. Kan (1981). Fatigue of composites under compression dominated spectrum loading. Advances in Aerospace Materials and Structures, Proceedings of ASME Conference, Washington, D.C.
12. Ratwani, M. M., and H. P. Kan (1983). Delamination based compression residual strength prediction model for composites. Proceedings of AIAA/ASME/ASCE/ASFS 24th Structures, Structural Dynamics and Materials Conference, Lake Tahoe, Nevada, 275-281.
13. Ratwani, M. M. (1980). Influence of penetrants used in X-ray radiography on compression fatigue life of graphite/epoxy laminates. Composites Technology Review, Vol. 2, No. 1.
14. Sendeckyj, G. P., G. E. Maddin, and G. Porter (1980). Damage documentation in composites by stereo radiography. Damage in Composite Materials. ASTM STP 775.
15. Masters, J. F., and K. L. Reifsnider (1980). An investigation of cumulative damage development in quasi-isotropic graphite/epoxy laminates. Damage in Composite Materials. ASTM STP 775.
16. Ratwani, M. M., and H. P. Kan (1980). Effect of stacking sequence on damage propagation and failure modes in composite laminates. Damage in Composite Materials. ASTM STP 775.
17. Ratwani, M. M., H. P. Kan, and A. H. McQuillan (1982). Damage accumulation in composites. Proceedings of the 1982 Joint Conference on Experimental Mechanics, SESA and JSME, Hawaii.
18. Phillips, E. P. (1979). Effects of truncation of a predominantly compression load spectrum on the life of a notched graphite/epoxy laminate. ASTM Symposium on the Fatigue of Fibrous Composite Materials, San Francisco, California.
19. Badaliane, R., H. P. Dill, and J. M. Potter (1982). Effects of spectrum variations on fatigue life of composites. Composite Materials Testing and Design (Sixth Conference). ASTM STP 787.